HHS Public Access

Author manuscript

Cancer Res. Author manuscript; available in PMC 2016 May 15.

Published in final edited form as:

Cancer Res. 2015 May 15; 75(10): 1936–1943. doi:10.1158/0008-5472.CAN-14-3303.

Manic Fringe Promotes A Claudin-Low Breast Cancer Phenotype through Notch-Mediated PIK3CG Induction

Shubing Zhang[1,2,*], **Wen-Cheng Chung**[1,*], **Guanming Wu**[3], **Sean E. Egan**[4], **Lucio Miele**[5], and **Keli Xu**[1,6]

[1]Cancer Institute, University of Mississippi Medical Center, Jackson, MS, USA

[2]State Key Laboratory of Medical Genetics and School of Life Sciences, Central South University, Changsha, Hunan, China

[3]Department of Medical Informatics & Clinical Epidemiology and Oregon Clinical & Translational Research Institute, Oregon Health & Science University, Portland, OR, USA

[4]Program in Developmental and Stem Cell Biology, The Hospital for Sick Children and Department of Molecular Genetics, University of Toronto, Toronto, Canada

[5]Stanley S. Scott Cancer Center, Louisiana State University Health Sciences Center and Louisiana Cancer Research Center, New Orleans, LA, USA

[6]Department of Neurobiology and Anatomical Sciences, University of Mississippi Medical Center, Jackson, MS, USA

Abstract

Claudin-low breast cancer (CLBC) is a poor prognosis disease biologically characterized by stemness and mesenchymal features. These tumors disproportionately affect younger patients and women with African ancestry, causing significant morbidity and mortality, and no effective targeted therapy exists at present. CLBC is thought to originate from mammary stem cells, but little is known on how or why these tumors express a stable epithelial-to-mesenchymal transition (EMT) phenotype, or what are the driving forces of this disease. Here we report that *Manic Fringe (Mfng)*, which encodes an O-fucosylpeptide 3-β-N-acetylglucosaminyltransferase known to modify EGF repeats in the Notch extracellular domain, is highly expressed in CLBC and functions as an oncogene in this context. We show that Mfng modulates Notch activation in human and mouse CLBC cell lines, as well as in mouse mammary gland. Mfng silencing in CLBC cell lines reduced cell migration, tumorsphere formation and in vivo tumorigenicity associated with a decrease in the stem-like cell population. Mfng deletion in the $Lfng^{flox/flox}$; MMTV-Cre mouse model, in which one-third of mammary tumors resemble human CLBC, caused a tumor subtype shift away from CLBC. We identified the phosphoinositide kinase Pik3cg as a direct transcriptional target of Mfng-facilitated RBPJκ-dependent Notch signaling. Indeed, pharmacological inhibition of PI3Kγ in CLBC cell lines blocked migration and tumorsphere

Correspondence: Keli Xu, Cancer Institute, University of Mississippi Medical Center, 2500 North State Street, Jackson, MS 39216, USA. Phone: (601)815-3083; Fax: (601)815-6806; kxu@umc.edu.

*Both authors contributed equally to this work

Conflict of Interest: The authors declare no conflict of interest.

formation. Taken together, our results define Mfng as an oncogene acting through Notch-mediated induction of Pik3cg. Further, they suggest that targeting PI3Kγ may prove beneficial for the treatment of claudin-low breast cancer subtype.

Keywords

Manic Fringe; Notch; claudin-low breast cancer; cancer stem cell; Pik3cg

Introduction

Gene expression profiling has been used to subclassify human breast cancer into at least six molecular subtypes, including Basal-like, Claudin-low, HER2-enriched, Luminal A, Luminal B and Normal-like. Claudin-low breast cancer (CLBC) shares features with mammary stem cells and CLBC cells have undergone epithelial-to-mesenchymal transition (EMT) (1,2). It is widely believed that cancer stem-like cells play a key role in tumor recurrence and metastasis. Also, accumulating evidence suggest that EMT promotes dissemination, and may itself promote “stemness” (3–5).

Notch signaling controls mammary stem cell self-renewal and differentiation, and may regulate EMT in breast cancer cells (6–9). Indeed, dysregulated Notch activation has been implicated in breast cancer, especially in subtypes showing features of mammary stem cells and EMT (10). As a result, Notch has emerged as a potential drug target for poor prognosis breast cancer. However, the role of Notch in different subtypes is not clear, nor is the specific Notch receptor(s), ligand(s), and the modulator(s) involved.

Lunatic Fringe (Lfng), *Manic Fringe (Mfng)*, and *Radical Fringe (Rfng)* encode a family of β3N-acteylglucosaminyl-transferases that are known to modify EGF repeats in the extracellular domains of Notch receptors, thereby modulating ligand-mediated Notch activation (11). We recently reported that Lfng controls self-renewal and differentiation of mammary stem/progenitor cells by restricting Notch activation, and *Lfng* deficiency cooperates with the *Met/Caveolin* gene amplification to induce basal-like breast cancer (BLBC) and, less frequently, CLBC (12). Analysis of human breast cancer data showed significantly reduced levels of LFNG expression in BLBC and in a subset of CLBC as compared to other subtypes. In contrast, expression of MFNG was significantly higher in CLBC. In this study, we performed loss-of-function analysis for *Mfng* in CLBC cell lines as well as mouse models to determine roles for Mfng in CLBC. We also identified a critical downstream effector of Mfng-modulated Notch signaling in this context.

Materials and Methods

Cells

MDA-MB231 was obtained from ATCC. Mouse cell line C0321 was established and maintained as previously described (13). Cells were resuscitated from early passage liquid nitrogen stocks and cultured less than 3 months before reinitiating cultures. Cells were tested negative for mycoplasma contamination.

Cell proliferation, migration, and tumorsphere assays, drug treatment, and xenograft experiment

Cell proliferation was assessed using CellTiter96 AQueous One Solution kit (Promega). Collective cell migration was measured in a wound-healing assay. Tumorespheres were cultured as previously described (13), and quantified using a cytometer (Celigo). For drug treatment, cells were incubated with AS-605240 (Selleck, S1410) at a final concentration of 10 μM. Xenografts were performed by injecting a total of 1×10^6 cells mixed with Matrigel (BD Bioscience) into the mammary fat pad in 4-week-old ICR/SCID mice (Taconic).

Western blot analysis and flow cytometry

Tissues or cells were lysed in RIPA buffer (Boston BioProducts) supplemented with protease and phosphatase inhibitors (Roche), and processed for Western blot analyses according to standard methodology. Flow cytometry was performed by standard procedures. Fluorescence was recorded using Gallios Flow Cytometer (Beckman Coulter) and analyzed with Kaluza flow cytometry analysis software. See supplementary methods for antibodies used for Western blot and flow cytometry analyses.

Mice

Mouse experiments were performed in accordance with a protocol approved by UMMC Institutional Animal Care and Use Committee. Wildtype, *Mfng*$^{-/-}$, *Lfng*$^{flox/flox}$*; MMTV-Cre*, and *Mfng*$^{-/-}$; *Lfng*$^{flox/flox}$*; MMTV-Cre* cohorts were maintained on the FVB background.

Histology, immunohistochemistry and X-Gal staining

Formalin-fixed paraffin-embedded tissues were processed for histological and immunohistochemical analysis by standard procedures (see supplementary methods for primary antibodies used for IHC). Representative images were acquired with a Nikon Eclipse 80i microscope. X-Gal staining in the mammary gland was performed as previously described (12).

Microarray gene expression analysis in xenografts

Total RNA was extracted from xenografts using RNeasy Mini Kit (Qiagen), and processed using the Ambion WT Expression Kit (Life Technologies) according to the manufacturer's instruction. The resultant biotinylated cRNA was fragmented and then hybridized to the GeneChip® Human Gene 1.0 ST Array (Affymetrix). The arrays were processed and scanned using the Affymetrix Model 450 Fluidics Station and Affymetrix Model 3000 7G scanner (Affymetrix). **.cel files generated by Affymetrix Expression Console Software were used for further analysis.

Gene expression analysis of human data set

Human breast cancer gene expression data set GSE18229 was downloaded from GEO (http://www.ncbi.nlm.nih.gov/geo/query/acc.cgi?acc=GSE18229). Expressions of MFNG, NOTCH4 and PIK3CG and clinical information of patient samples were extracted by an in-house Java parser. Averaged values were used if more than one probe was mapped to same

genes. All plots and analyses were performed using R (http://www.r-project.org). p value was calculated by comparing expression means across all subtypes.

CHIP, luciferase reporter assays

ChIP assay was performed using EZ-ChIP kit (Millipore). Briefly, MDA-MB231 cells were treated with 1% formaldehyde, neutralized, and resuspended in SDS lysis buffer for chromatin fragmentation with sonication (ultrasonic processor GE130). Sheared chromatin was diluted and then immunoprecipitated with anti-RBPJκ (Abcam, ab25949) or normal IgG. DNA from immuneprecipitates was recovered by reversing the crosslinking and digestion with proteinase K, and then PCR amplified (see supplementary methods for primer sequences).

The PIK3CG promoter reporter was prepared by cloning the upstream region of PIK3CG gene (−1131-> −1) into the pGL3 vector (Promega). The mutagenesis of RBPJκ-binding sites was introduced by replacing the sequence with an NheI restriction site. All the clones are confirmed by sequencing. MDA-MB231 cells were co-transfected with PIK3CG promoter reporter and Renilla luciferase plasmids, and harvested 48 h post transfection. Luciferase activities were measured with Dual-Luciferase Reporter Assay System (Promega) using GloMax 96 Microplate Luminometer (Promega). Each reporter activity was normalized with corresponding Renilla activity.

shRNA, quantitative RT-PCR

The MFNG-shRNA construct targeting 5′-GTGCTGGCTTCTGCATCAATCGCAAACTG-3′ sequences of *MFNG* gene was purchased from Origene. MDA-MB231 and C0321 cells were transfected with the shRNA or scrambled control plasmid using FuGENE 6 Transfection Reagent (Promega). Stable cell lines expressing shRNA were generated by selection with Puromycin. For quantitative RT-PCR, total RNA was extracted using RNeasy Mini kit and reverse transcribed using iScript cDNA synthesis kit (Bio-rad). PCR was performed using QuantiTect SYBR Green PCR Kit (Qiagen) and quantitated with BioRad CFX96 qPCR System (see supplementary methods for primer sequences).

Statistics

Unpaired two-tailed t-tests were performed for two group comparisons, and p value of 0.05 or less was considered statistically significant.

Accession codes

The microarray data have been deposited in the NCBI Gene Expression Omnibus (GEO) under accession number GSE62481.

Results

Modulation of Notch activation by Mfng in CLBC cell lines and in the mouse mammary gland

In a survey for Notch pathway gene expression in a human breast cancer data set, GSE18229 (1), we found that MFNG expression is significantly higher in CLBC as compared to other subtypes (p-value < 2e–16 from ANOVA, Fig. 1A). Interestingly, there is a positive correlation between MFNG and NOTCH4 expressions across all subtypes (Fig. 1B). Claudin-low tumors from *Lfng*$^{fl/fl}$*; MMTV-Cre* mice also showed elevated Mfng expression (12). Moreover, using SAM analysis on 385 mouse mammary tumor samples from 27 models, Mfng and Notch4 are found to be expressed at significantly higher levels in claudin-low subtype tumors than in tumors from all other subtypes (14). Thus, Mfng is up-regulated in CLBC in both humans and mice.

To determine the function of Mfng in CLBC, we performed *MFNG*-knockdown in MDA-MB231, a human breast cancer cell line with a claudin-low gene expression signature (1,2). To this end, we selected a polyclonal cell population transfected with a MFNG shRNA expression vector. This population showed a 40% decrease in MFNG mRNA expression as well as a decrease in Notch1 and Notch4 protein accumulation as compared to control cells (Fig. 1C and D). Importantly, the size of Notch1 and Notch4 fragments detected are consistent with Notch intracellular domains (N-ICD), suggesting reduced Notch1 and Notch4 activation in these cells. Indeed, *MFNG*-knockdown cells expressed lower levels of a canonical Notch target gene, HEY1 (Fig. 1C). We also knocked down *Mfng* in a murine Claudin-low cell line, C0321 (13). In this case, shRNA-expressing cells showed a 60% reduction in Mfng mRNA and decreased N4-ICD accumulation, but increased level of N1-ICD (Fig. 1C and D). shMfng C0321 cells showed decreased mRNA levels of Hes1 and Hes5, but increased Hey1 expression (Fig. 1C).

We next examined *Mfng* expression in the mouse mammary gland using a *Mfng*$^{\beta\text{-}Geo/+}$ reporter strain (Supplementary Fig. 1). Weak *Mfng* expression is noted at the branching sites of epithelial ducts in the pubescent gland. Interestingly, *Mfng* expression is up-regulated dramatically during post-weaning involution. Next we analyzed Notch protein levels in mammary tissue from *Mfng* null mice (*Mfng*$^{\beta\text{-}Geo/\beta\text{-}Geo}$, referred to as *Mfng*$^{-/-}$). A dramatic decrease in N4-ICD and increase in N1- and N3-ICD were noted in the *Mfng*$^{-/-}$ mammary gland during involution, but not during puberty. Interestingly, deletion of *Mfng* in the *Lfng*$^{flox/flox}$*; MMTV-Cre* mice caused a decrease in N4-ICD accumulation during puberty (Fig. 1D). Thus, modulation of Notch1 activation by Mfng is context-dependent: enhanced in MDA-MB231, but inhibited in C0321 and in mouse mammary gland during involution. Mfng appears to enhance Notch4 activation in both human and mouse CLBC cell lines, as well as in the mouse mammary gland.

Mfng regulates self-renewal of cancer stem-like cells and cell migration in CLBC cell lines

Knockdown of *Mfng* had no effect on the growth of MDA-MB231 or C0321 cells cultured on plastic (Supplementary Fig. 2), however, it dramatically decreased tumorsphere-forming capacity of both lines (Fig. 2A). Flow cytometry analysis revealed a diminished population

of $CD44^{+}CD24^{low+}$ cells (from 9.18% to 3.33%) in the *MFNG*-knockdown MDA-MB231 cells (Fig. 2C). This population was shown to have enriched breast cancer stem-like cells and to express N1-ICD as well as Notch target genes (15). Knockdown of *Mfng* in C0321 caused a dramatic decrease in $CD44^{+}CD24^{-}$ and $CD44^{+}CD24^{low+}$ populations, again, both of which are enriched for cancer stem-like cells (16) (Fig. 2C). *Mfng*-knockdown cells showed a lower migration rate in the "wound healing" assay (Fig. 2D). Finally, xenograft of the *MFNG*-knockdown MDA-MB231 cells resulted in diminished tumor growth compared to the control line (n=9, p-value = 0.0002, Fig. 2B). Taken together, these results indicate that Mfng promotes accumulation of stem-like tumor-initiating cells and cell migration, as well as enhancement of tumor growth *in vivo*.

Mfng influences breast cancer subtypes in the $Lfng^{flox/flox}$; MMTV-Cre mouse model

Mfng may regulate mammary epithelial differentiation through modulation of Notch. Indeed, the mature $Mfng^{-/-}$ mammary gland showed increased levels of the luminal cell marker cytokeratin 8 (CK8), as well as basal cell marker CK14, associated with a modest decrease in ERα level and a dramatic decrease in PRβ (Fig. 3A). Despite this, $Mfng^{-/-}$ mice showed normal lactation and post-weaning involution, and no mammary tumor formation. To test for a role of Mfng in CLBC pathogenesis, we crossed *Mfng* null mice to the $Lfng^{flox/flox}$*; MMTV-cre* model, which develop basal like (~2/3) and claudin-low/spindle cell (~1/3) mammary tumors (12). Deletion of *Mfng* in this model caused increased CK8 expression as well as decreased levels of a stem cell marker, Aldh1 (Fig. 3A). Unexpectedly, some of the $Mfng^{-/-}$; $Lfng^{flox/flox}$*; MMTV-cre* mice succumbed to lymphoma prior to the onset of mammary tumor formation, likely due to the loss of both *Lfng* and *Mfng* in B- and T-cells. Nevertheless, we were able to harvest mammary tumors from some of these mice. Interestingly, two of three were adenosquamous carcinomas and one showed histology resembling the basal-like tumor from the $Lfng^{flox/flox}$*; MMTV-cre* model. The Claudin-low subtype, which often displays spindloid histology (12), was not found (Fig. 3B). Unlike basal-like and claudin-low tumors, the adenosquamous carcinoma showed nuclear staining of ERα and PR in some cells (Fig. 3C). Adenosquamous carcinoma was never found in more than 50 tumors collected from $Lfng^{flox/flox}$*; MMTV-cre* mice during our previous and present studies. Thus, deletion of *Mfng* caused squamous differentiation at the expense of claudin-low subtype. Compared with basal-like tumors, claudin-low tumors and cell lines from the $Lfng^{flox/flox}$*; MMTV-cre* mice express more Notch4 and less Notch1 (12,13). Consistent with a subtype shift away from claudin-low, we observed a decrease in Notch4 and increase in Notch1 protein accumulation in *Mfng*-knockdown C0321 cells (Fig. 1D).

Pik3cg is a direct target of Mfng-enhanced Notch signaling in CLBC

To identify downstream mediators of Mfng, we performed microarray gene expression analysis on 6 xenograft tumors, 3 each from control and *MFNG* shRNA-expressing MDA-MB231 cells. One of the most down-regulated genes in *MFNG* knockdown tumors is *PIK3CG*, which appears to be a hub in the reactome functional interaction network of differentially expressed genes (Fig. 4A, Supplementary Table 1, and Supplementary Fig. 3). Encoding the γ catalytic subunit of phosphatidylinositol-4,5-bisphosphate 3-kinase, *PIK3CG* has recently been shown to promote breast cancer growth and metastasis (17,18). We verified that knockdown of *Mfng* caused a dramatic decrease in Pik3cg level, as well as

reduced Akt phosphorylation in CLBC cells (Fig. 4A). Since knockdown of *Mfng* decreased Notch1 and Notch4 activation in MDA-MB231, we tested whether Mfng controls Pik3cg expression through Notch1 or Notch4. Indeed, overexpression of N1-ICD and/or N4-ICD resulted in increased Pik3cg protein level in MDA-MB231 cells (Fig. 4B). The *PIK3CG* gene promoter harbors multiple consensus Rbpjκ-binding sites, including two in a region less than 1 Kb upstream of the start codon. To test for Rbpjκ-binding to these sequences, we performed chromatin immunoprecipitation (ChIP). Sequences surrounding both sites were amplified from the Rbpjκ-chromatin complex. Luciferase reporter assay using constructs from the *PIK3CG* promoter, including one or both Rbpjκ-binding sites revealed that both sites are required for the Notch-ICD dependent transcriptional activation (Fig. 4B). Thus, *Pik3cg* is a direct target of Rbpjκ-dependent Notch signaling in CLBC cells. Moreover, PIK3CG expression positively correlates with MFNG expression in human breast tumors (p-value < 2.2e–16, Fig. 4C and Supplementary Table 2). Also, PIK3CG, but not PIK3CA, is highly expressed in CLBC subtype (Fig. 4C, and data not shown). Interestingly, Notch pathway activation conferred resistance to PI3K inhibitors in a chemical genetic screen on human cancer cell lines (19), consistent with our finding that Notch activation up-regulates *Pik3cg* expression.

Next we tested for the importance of Pik3cg in CLBC cells using a selective PI3Kγ inhibitor, AS-605240. “Wound healing” assays showed that inhibition of PI3Kγ activity almost completely blocked the migration of C0321 cells, and significantly attenuated that of MDA-MB231 (Fig. 4D). The same concentration of AS-605240 had no effect on growth of MDA-MB231, and did not impede C0321 proliferation until 2 days after treatment (Supplementary Fig. 4), indicating that failed “wound healing” is not due to inhibition of cell growth. Interestingly, treatment of MDA-MB231 cell line with AS-605240 for 3 days caused a decrease of 17.2±1.8% in the $CD44^{+}CD24^{low+}$ cells. To avoid complication of the inhibitory effect of AS-605240 on cell proliferation, we performed flow cytometry in C0321 cells after treatment for only 2 days. Again, AS-605240 treated C0321 line showed modest but consistent reduction (13.6±1.9%, $p<0.05$) in the $CD44^{+}CD24^{-}$ cancer stem cell-enriched population (Fig. 4D). Indeed, treatment with AS-605240 resulted in a dramatically decreased capacity of tumorsphere formation in both cell lines (Fig. 4D). Taken together, PI3Kγ activity is not only required for cell migration, but also contributes to maintenance of claudin-low cancer stem-like cells.

Discussion

Multiple Notch receptors are expressed in the developing mammary gland and in breast cancer, and individual Notch receptors may exert distinct roles in different mammary cell types. For instance, Notch4 has been shown to regulate self-renewal of stem or bipotential progenitor cells (8,20), whereas Notch3 is reported to function in luminal progenitor cells (8,21). In this study, we found that MFNG expression in breast cancer is highly correlated with expression of NOTCH4, but not with expression of other Notch receptors. In addition, knockdown of *Mfng* in human and mouse CLBC cell lines consistently decreased Notch4 activation, while deletion of *Mfng* in the mouse mammary gland resulted in decreased Notch4 activation during involution. Thus, it appears that Mfng primarily controls Notch4-

mediated signaling in mammary stem cells, which is thought to be the cell-of-origin for CLBC.

Mfng expression in the mammary gland is dramatically up-regulated during post-weaning involution. Interestingly, deletion of *Mfng* caused increased activation of Notch1 and Notch3, and decreased Notch4 expression/activation during involution. In this context, Mfng may regulate parity-induced stem cell activity through differential regulation of Notch receptor activation. The involuting mammary gland microenvironment can promote tumor progression in some cases (22). To some extent, the microenvironment of claudin-low tumors is reminiscent of that of postpartum mammary glands, where Mfng may enhance self-renewal of stem-like cells and promote EMT.

Loss of *Mfng* on the $Lfng^{flox/flox}$*; MMTV-cre* background induced formation of adenosquamous carcinoma at the expense of claudin-low mammary tumors. In this case, deletion of both *Lfng* and *Mfng* in the mammary gland caused dramatically decreased activation of multiple Notch receptors (Fig.1D), suggesting that overall reduction in Notch signaling may lead to squamous differentiation of the mammary epithelium. Interestingly, inactivating mutations in Notch pathway genes have been identified in squamous cell carcinoma of other tissues including head and neck, lung and bladder (23).

Pik3cg is aberrantly expressed in many invasive human breast tumors and its expression level correlates with metastatic potential of breast cancer cell lines (18). Here we demonstrate that Pik3cg is a downstream effector of Mfng-facilitated Notch activation. Previous studies indicate that Pik3cg may promote migration and invasion of breast cancer cells, while inhibiting anoikis (17,18). Our results suggest that Pik3cg contributes to breast cancer aggressiveness not only by promoting cell migration, but also by maintaining cancer stemness.

In conclusion, this study revealed a novel oncogenic role for Mfng in CLBC. Our discovery of a specific role of Mfng-controlled Notch signaling in CLBC provides new insights into the regulation of cancer stem cells in specific breast cancer subtypes. Finally, identification of *Pik3cg* as a Notch target prompts a PI3Kγ-targeting strategy for treatment of CLBC and perhaps other poor prognosis breast cancers, and opens a new avenue to search for prognostic biomarkers for breast cancers based on expression of MFNG, NOTCH and PIK3CG.

Supplementary Material

Refer to Web version on PubMed Central for supplementary material.

Acknowledgements

This work was supported by NIH grant (R21CA175136) to KX. LM was supported by NIH grant P01CA166009. SEE's lab was supported by funding from the Cancer Research Society. The authors thank the UMMC Flow Cytometry Core and Molecular and Genomics Core staff for their expertise.

References

1. Prat A, Parker JS, Karginova O, Fan C, Livasy C, Herschkowitz JI, et al. Phenotypic and molecular characterization of the claudin-low intrinsic subtype of breast cancer. Breast cancer research : BCR. 2010; 12:R68. [PubMed: 20813035]
2. Prat A, Karginova O, Parker JS, Fan C, He X, Bixby L, et al. Characterization of cell lines derived from breast cancers and normal mammary tissues for the study of the intrinsic molecular subtypes. Breast cancer research and treatment. 2013; 142:237–255. [PubMed: 24162158]
3. Scheel C, Weinberg RA. Cancer stem cells and epithelial-mesenchymal transition: concepts and molecular links. Seminars in cancer biology. 2012; 22:396–403. [PubMed: 22554795]
4. Mani SA, Guo W, Liao MJ, Eaton EN, Ayyanan A, Zhou AY, et al. The epithelial-mesenchymal transition generates cells with properties of stem cells. Cell. 2008; 133:704–715. [PubMed: 18485877]
5. Hollier BG, Evans K, Mani SA. The epithelial-to-mesenchymal transition and cancer stem cells: a coalition against cancer therapies. Journal of mammary gland biology and neoplasia. 2009; 14:29–43. [PubMed: 19242781]
6. Bouras T, Pal B, Vaillant F, Harburg G, Asselin-Labat ML, Oakes SR, et al. Notch signaling regulates mammary stem cell function and luminal cell-fate commitment. Cell stem cell. 2008; 3:429–441. [PubMed: 18940734]
7. Lombardo Y, Faronato M, Filipovic A, Vircillo V, Magnani L, Coombes RC. Nicastrin and Notch4 drive endocrine therapy resistance and epithelial-mesenchymal transition in MCF7 breast cancer cells. Breast cancer research : BCR. 2014; 16:R62. [PubMed: 24919951]
8. Raouf A, Zhao Y, To K, Stingl J, Delaney A, Barbara M, et al. Transcriptome analysis of the normal human mammary cell commitment and differentiation process. Cell stem cell. 2008; 3:109–118. [PubMed: 18593563]
9. Leong KG, Niessen K, Kulic I, Raouf A, Eaves C, Pollet I, et al. Jagged1-mediated Notch activation induces epithelial-to-mesenchymal transition through Slug-induced repression of E-cadherin. The Journal of experimental medicine. 2007; 204:2935–2948. [PubMed: 17984306]
10. Harrison H, Farnie G, Brennan KR, Clarke RB. Breast cancer stem cells: something out of notching? Cancer research. 2010; 70:8973–8976. [PubMed: 21045140]
11. Haines N, Irvine KD. Glycosylation regulates Notch signalling. Nat Rev Mol Cell Biol. 2003; 4:786–797. [PubMed: 14570055]
12. Xu K, Usary J, Kousis PC, Prat A, Wang DY, Adams JR, et al. Lunatic Fringe deficiency cooperates with the Met/Caveolin gene amplicon to induce basal-like breast cancer. Cancer Cell. 2012; 21:626–641. [PubMed: 22624713]
13. Zhang S, Chung WC, Miele L, Xu K. Targeting Met and Notch in the Lfng-deficient, Met-amplified triple-negative breast cancer. Cancer biology & therapy. 2014; 15:633–642. [PubMed: 24556651]
14. Pfefferle AD, Herschkowitz JI, Usary J, Harrell JC, Spike BT, Adams JR, et al. Transcriptomic classification of genetically engineered mouse models of breast cancer identifies human subtype counterparts. Genome biology. 2013; 14:R125. [PubMed: 24220145]
15. Azzam DJ, Zhao D, Sun J, Minn AJ, Ranganathan P, Drews-Elger K, et al. Triple negative breast cancer initiating cell subsets differ in functional and molecular characteristics and in gamma-secretase inhibitor drug responses. EMBO molecular medicine. 2013; 5:1502–1522. [PubMed: 23982961]
16. Al-Hajj M, Wicha MS, Benito-Hernandez A, Morrison SJ, Clarke MF. Prospective identification of tumorigenic breast cancer cells. Proceedings of the National Academy of Sciences of the United States of America. 2003; 100:3983–3988. [PubMed: 12629218]
17. Brazzatti JA, Klingler-Hoffmann M, Haylock-Jacobs S, Harata-Lee Y, Niu M, Higgins MD, et al. Differential roles for the p101 and p84 regulatory subunits of PI3Kgamma in tumor growth and metastasis. Oncogene. 2012; 31:2350–2361. [PubMed: 21996737]
18. Xie Y, Abel PW, Kirui JK, Deng C, Sharma P, Wolff DW, et al. Identification of upregulated phosphoinositide 3-kinase gamma as a target to suppress breast cancer cell migration and invasion. Biochemical pharmacology. 2013; 85:1454–1462. [PubMed: 23500535]

19. Muellner MK, Uras IZ, Gapp BV, Kerzendorfer C, Smida M, Lechtermann H, et al. A chemical-genetic screen reveals a mechanism of resistance to PI3K inhibitors in cancer. Nature chemical biology. 2011; 7:787–793.
20. Harrison H, Farnie G, Howell SJ, Rock RE, Stylianou S, Brennan KR, et al. Regulation of breast cancer stem cell activity by signaling through the Notch4 receptor. Cancer Res. 2010; 70:709–718. [PubMed: 20068161]
21. Lafkas D, Rodilla V, Huyghe M, Mourao L, Kiaris H, Fre S. Notch3 marks clonogenic mammary luminal progenitor cells in vivo. The Journal of cell biology. 2013; 203:47–56. [PubMed: 24100291]
22. Lyons TR, O'Brien J, Borges VF, Conklin MW, Keely PJ, Eliceiri KW, et al. Postpartum mammary gland involution drives progression of ductal carcinoma in situ through collagen and COX-2. Nature medicine. 2011; 17:1109–1115.
23. Xu K, Bagli DJ, Egan SE. NOTch Just a Bladder Control Problem. Cancer cell. 2014; 26:452–454. [PubMed: 25314075]

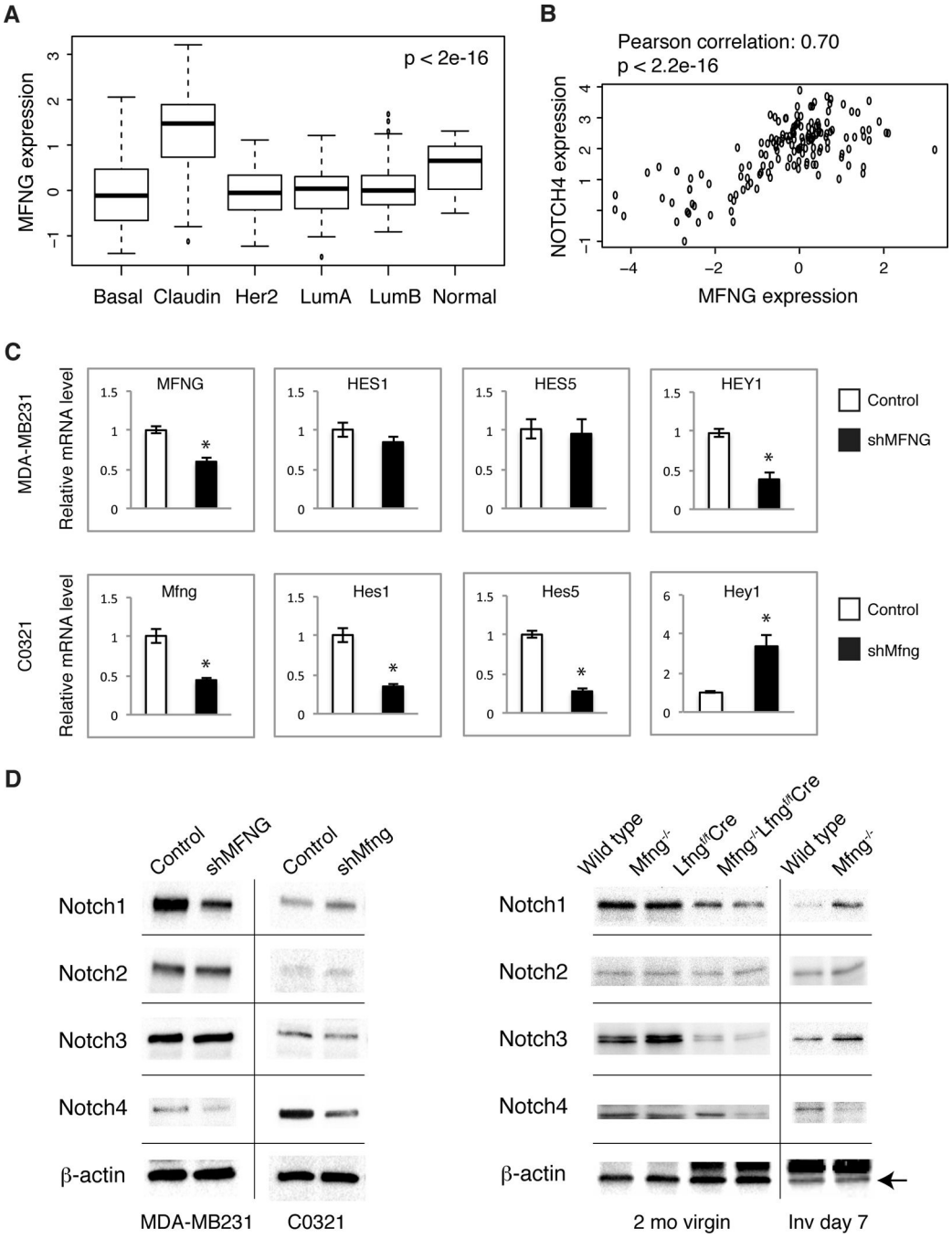

Figure 1.

Mfng is highly expressed in human CLBC and modulates Notch activation in CLBC cell lines and in the mouse mammary gland. **A**, Mean expression values of MFNG from the human breast cancer data set GSE18229. Basal (Basal-like), Claudin (Claudin-low), Her2 (Her2-enriched), LumA (Luminal A), LumB (Luminal B) and Normal (Normal breast-like) are six molecular subtypes. **B**, Scatterplot for MFNG and NOTCH4 expressions in human breast cancers from GSE18229. **C**, Quantitative RT-PCR for Mfng and Notch target genes Hes1, Hes5, and Hey1 in MDA-MB231 and C0321 cell lines stably expressing Mfng-

shRNA or scrambled control. * $p < 0.05$. **D**, Western blot analysis for Notch receptors in the control and shMfng cell lines, and in mouse mammary tissues of indicated genotypes and stages.

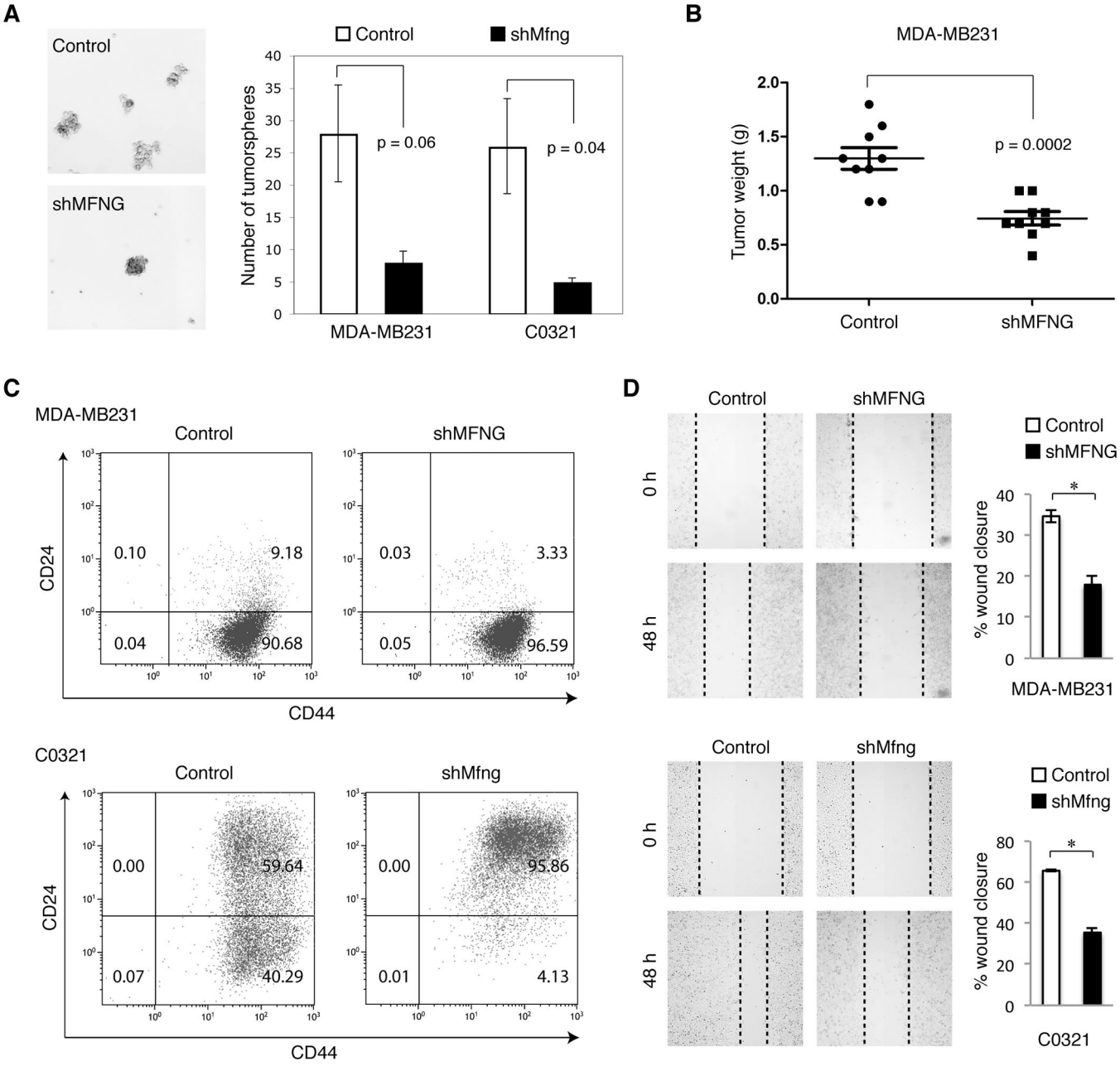

Figure 2.

Knockdown of Mfng in CLBC cell lines caused a decreased number of cancer stem-like cells, reduced cell migration, and diminished growth of xenografts. **A**, Representative photomicrographs of tumorspheres formed in 3D cultures of the control and shMFNG MDA-MB231 cells, and quantification of tumorspheres formed per 2,000 cells of control or shMfng cell lines. **B**, Weights of xenograft tumors from 1×10^6 control or shMFNG MDA-MB231 cells at 8 wk post-injection (n=9). **C**, Representative CD24/CD44 flow cytometry profiles of the control and shMFNG MDA-MB231 cell lines, control and shMfng C0321 cell lines. **D**, Representative images and quantification of the wound healing assays in the control and shMfng cell lines. *$p < 0.05$.

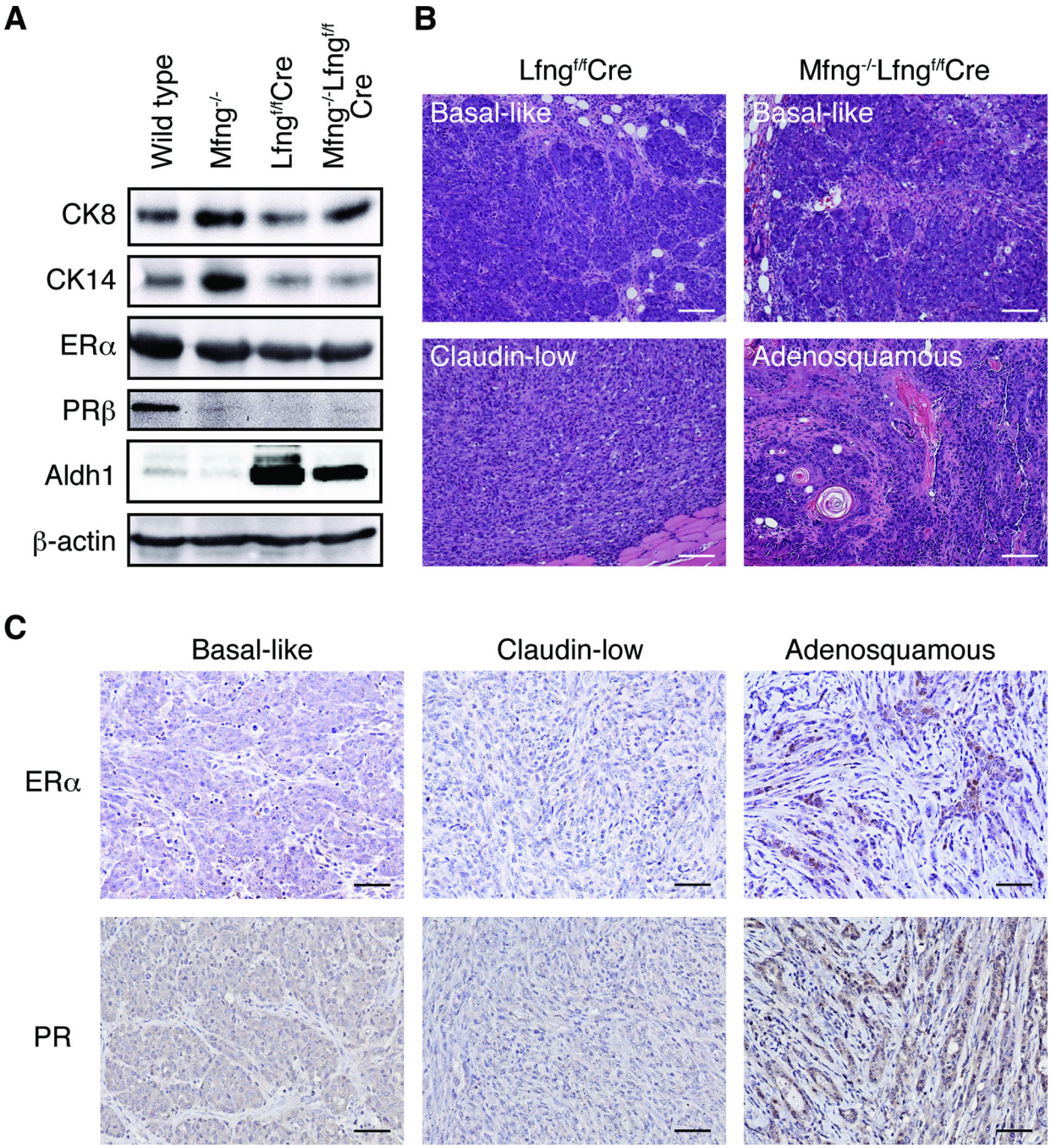

Figure 3.

Deletion of *Mfng* in the *Lfng*$^{flox/flox}$*; MMTV-Cre* mouse model altered mammary tumor subtypes. **A**, Western blot analyses for CK8, CK14, ER, PR, and Aldh1 in the mammary tissue from age-matched mice of indicated genotypes. **B**, Representative H&E staining of different mammary tumor subtypes from the *Lfng*$^{flox/flox}$*; MMTV-Cre* and *Mfng*$^{-/-}$*; Lfng*$^{flox/flox}$*; MMTV-Cre* mice. **C**, Representative photomicrographs of anti-ERα and anti-PR immunostaining in three subtypes of mammary tumors shown in B. Scale bars: 100 μm in B; 50 μm in C.

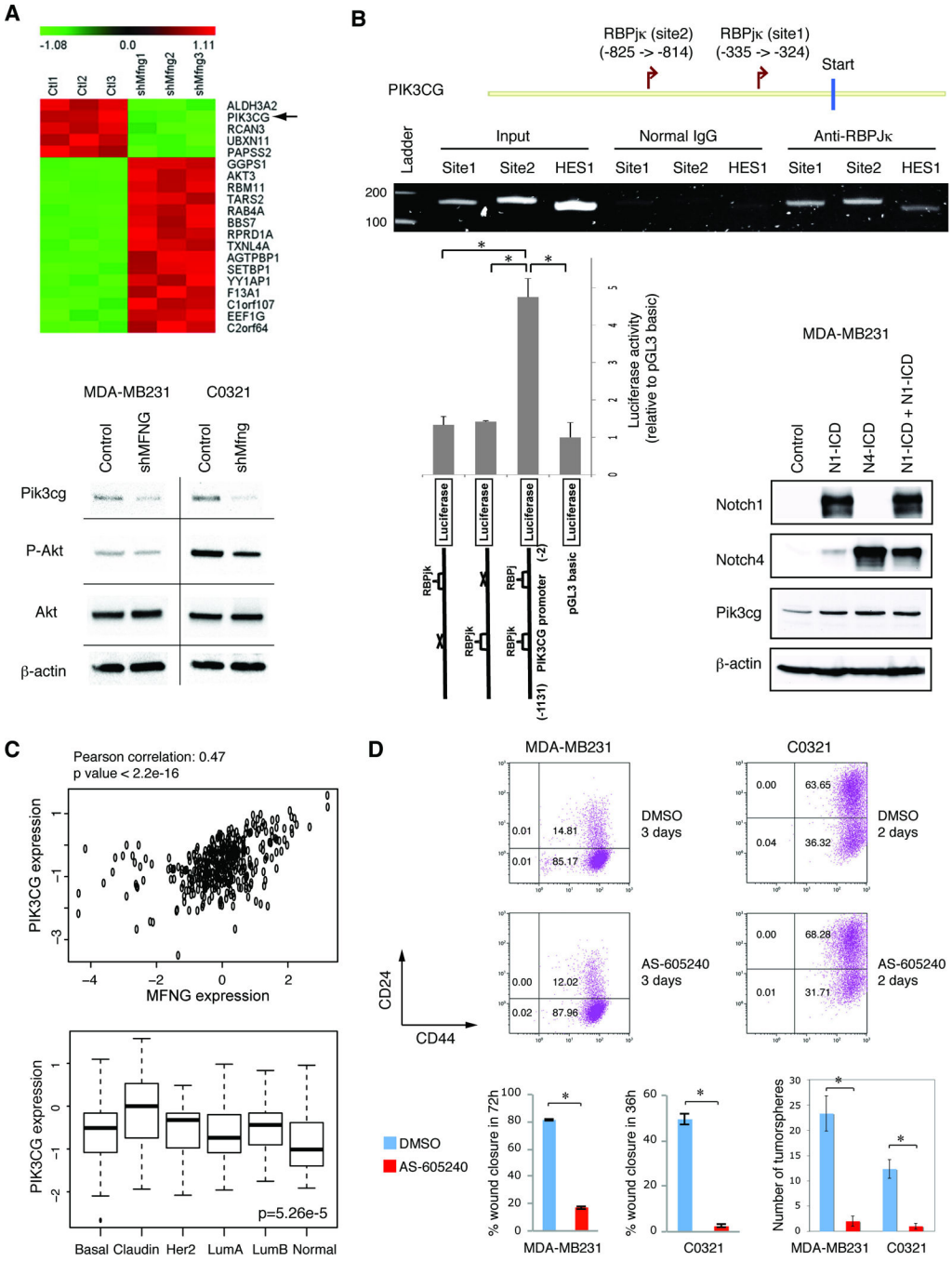

Figure 4.

Pik3cg is a direct target of Mfng-enhanced, Rbpjκ-dependent, Notch signaling in CLBC. **A**, Top differentially expressed genes in xenografts from injections of control vs shMFNG MDA-MB231 cells, and Western blot analysis for Pik3cg, Phospho-Akt, and total Akt in the control and shMfng cell lines. **B**, ChIP analysis of the *PIK3CG* promoter in MDA-MB231 cells showing endogenous RBPJκ binding at two sites. *HES1* promoter is included as a positive control. Luciferase reporter of the *PIK3CG* promoter with two intact RBPJκ–binding sites is activated endogenously in MDA-MB231 cells. Data were derived from three

independent experiments. *p < 0.05. Also shown is Western blot analysis for Notch1, Notch4, and Pik3cg in MDA-MB231 cells with overexpression of N1-ICD and/or N4-ICD. **C**, Scatterplot for MFNG and PIK3CG expressions in human breast cancer, and mean expression values of PIK3CG in six molecular subtypes of human breast cancer (data from GSE18229). **D**, Representative CD24/CD44 flow cytometry profiles of the MDA-MB231 and C0321 cells treated with AS-605240 (or DMSO as control) for 3 and 2 days, respectively. Also shown are measurement of cell migration by wound healing assay in MDA-MB231 and C0321 cells treated with AS-605240 or DMSO, and quantification of tumorspheres formed per 2,000 cells of MDA-MB231 and C0321 treated with AS-605240 or DMSO. *p < 0.05.